

Functional Effects of Island-Distribution of Mid-cardiomyocytes on Re-entrant Excitation Waves in the KCNQ1-linked Short QT Syndrome

Cunjin Luo¹, Kuanquan Wang¹, Henggui Zhang^{1,2}

¹School of Computer Science and Technology, Harbin Institute of Technology, Harbin, China

²School of Physics and Astronomy, the University of Manchester, Manchester, United Kingdom

Abstract

It is recognized that specific mutations in ion channels responsible for cellular repolarization underlie various forms of the short QT syndrome (SQTs). However, the functional effects of the intrinsic spatial heterogeneities, such as island-distribution of mid-cardiomyocytes (M island) in cardiac tissue on the electrical instability in SQTs are poorly understood. In this study, the effect of M island on the generation and maintenance of re-entrant waves was investigated by using ten Tusscher et al. model. This model was extended to include a description of the KCNQ1-linked short QT syndrome (SQT2). A two dimensional (2D) tissue model, representing a transmural slice, comprised of 100×400 cells, among which 35% cells were mid-cardiomyocytes, either distributed in island form (M island) or continuous band (M band), 25% were endocardial and the rest were epicardial cells. The simulation data predicted that in SQT2 re-entry was more easily initiated and sustained in the M island model than in the M band model. It illustrated the important role of the intrinsic spatial electrical heterogeneities of cardiac tissue in the increased incidence of ventricular fibrillation associated with short QT syndrome.

1. Introduction

Re-entrant excitation waves in the cardiac disease may arise from the intrinsic spatial heterogeneities of cardiac wall leading to functional electrical instability, and greatly enhance the probability that triggers re-entrant excitation waves, which is subsequently thought to lead to ventricular tachycardia (VT) and ventricular fibrillation (VF) [1]. Genetic short QT syndrome (SQTs) is associated with an increased risk of VT and VF arrhythmias, possibly due to high-frequency re-entrant excitation waves. To date, several variants of SQTs have been identified, involving gain-in-function mutations. These mutations involve different potassium channel proteins that control repolarization. One of SQTs, SQT2 variant, has been associated with mutations in KCNQ1, the gene responsible for the α -subunit of the I_{Ks} channel

[2,3]. Although the KCNQ1 mutation is causally linked to the QT interval shortening, an increased transmural heterogeneity of action potential duration (APD) and effective refractory period (ERP), increased tissue's vulnerability to the genesis of re-entry, and sustained re-entry [4], the precise mechanisms leading to increased arrhythmic risk in SQT2 are not completely known.

Increased spatial transmural heterogeneity of cardiac tissue in SQT2 causes to ventricular cells to repolarize at different rates, which has been postulated to function as a substrate for re-entry phenomena [4]. Moreover, spatial heterogeneities are present in various forms, one of which is the presence of mid-cardiomyocytes, roughly distributed in island form (M island) that varies in spatial extent across the heart [1]. These islands consist of mid-cardiomyocytes that have distinct electrophysiological properties, most notably prolonged APD. Our group previously undertook studies to investigate the SQT2 syndrome [4], but did not address the functional effects of island distribution of mid-cardiomyocytes on the re-entrant excitation waves. The extent to which M island distribution may functionally influence transmural dispersion of repolarization or arrhythmogenesis in SQT2 remains unclear.

In order to focus on the potential mechanism detailed above, in this paper, we developed a two dimensional (2D) virtual transmural heterogeneous wall. This virtual wall was used to demonstrate potential effects of M island distribution on re-entrant excitation waves in the SQT2 syndrome.

2. Methods

In order to simulate re-entrant excitation waves in a 2D heterogeneous virtual cardiac wall, the electrical activity of cells was described by using the biophysically detailed ten Tusscher *et al.* dynamic model for cellular action potentials [5]. The heterogeneity of the ventricular models was included through the transient outward potassium current (I_{to}) and the slow delayed potassium rectifier current (I_{Ks}) [5]. Ignoring the microscopic nature of cell structure in the heart, the dynamics of the tissue

was described by the following reaction-diffusion-type partial differential equation (PDE):

$$C_m \frac{\partial V}{\partial t} = -(I_{ion} + I_{stim}) + \nabla \cdot (D \nabla V) \quad (1)$$

where V is the membrane potential, C_m is the cell capacitance per unit surface area, ∇ is gradient operator, D is the diffusion coefficient, describing the tissue conductivity. For D , we use $D = 0.0008 \text{ cm}^2 \text{ ms}^{-1}$ in 2D simulations to obtain a maximum planar conduction velocity (CV) of 60 cm s^{-1} , close to the 70 cm s^{-1} velocity of conduction along the fibre direction in human myocardium [6]. D is homogeneous except for a 5-fold decrease at the EPI-M border [4,7].

In our simulations, we considered a 2D virtual rectangular tissue which took the transmural dimension to be 15 mm , while the other dimension was taken to be 60 mm . As we focus here on the effects of regional heterogeneities in transmural geometry, the possible diversity of M island/band size is referenced from the literature [9,10]. We have taken geometrical distributions of heterogeneity introduced by subdividing into three domains, among which 35% were mid-cardiomyocytes (M), either distributed in island form or continuous band form (Fig. 1A is M band, Fig. 1B is M island), 25% were endocardial (ENDO) cells and the rest were epicardial (EPI) cells [4,8,11,12].

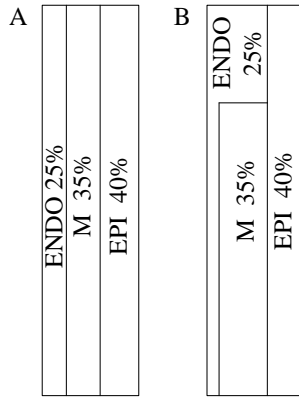


Fig. 1. Geometrical distribution for heterogeneous ventricular wall. A: M band. B: M island.

In order to simulate the SQT2, we took into account of two main situations: wild type (WT), and Homozygous mutant expression with reduced KCNE1 (HomKCNE1red). According to reference [4], I_{Ks} formulations were modified as follows:

$$I_{Ks} = g_{Ks} x_s^2 (V_m - E_{Ks}) \quad (2)$$

WT:

$$\frac{dx_s}{dt} = \frac{(x_{s,\infty} - x_s)}{\tau_{x_s}} \quad (3)$$

$$x_{s,\infty} = \frac{1}{1 + e^{(-5.9 - V_m)/17.4}} \quad (4)$$

HomKCNE1red:

$$\frac{dx_s}{dt} = \frac{(x_{s,\infty} - x_s)}{0.32 * \tau_{x_s}} \quad (5)$$

$$x_{s,\infty} = \frac{1}{1 + e^{(-24.0 - V_m)/16.0}} \quad (6)$$

where g_{Ks} is the channel maximal conductance, x_s is the activation variable, V_m is the cell membrane potential, E_{Ks} is the channel equilibrium potential and τ_{x_s} is the voltage-dependent time constant of activation. For details of other equations please see the ten Tusscher *et al.* reference [5].

A forward Euler method was used for the temporal discretization of differential equations, and discrete element method was applied for spatial discretization. In simulations, we set the basic cycle length (BCL) of 800 ms and, and took a spatial discretization of 0.15 mm and a time step of 0.02 ms. Re-entrant excitation waves in a 2D tissue model were initiated by a standard S1-S2 protocol. The first basic stimulus (S1, amplitude: -52 pA/pF, duration: 1 ms) was applied to the endocardial surface of the ENDO layer to evoke a planar propagating wavefront towards the EPI layer. A time delay after the 10th S1 stimulus for electrical variable stabilization, the second stimulus (S2, amplitude: -104 pA/pF, duration: 3 ms), which mimics a premature stimulus, was applied to a local area of the tissue to produce a unidirectional conduction leading to genesis of re-entrant excitation waves if it fell in the vulnerable window.

3. Results

In Fig. 2, the spatial and temporal evolution of the membrane potentials in WT (Fig. 2A, B) and SQT2 HomKCNE1red (Fig. 2C, D) conditions are shown for M band (Fig. 2A, C) and M island (Fig. 2B, D) distributions considered. The tissue was stimulated with S1-S2 protocol and the second premature test stimulus produced unidirectional conduction leading to genesis of re-entrant excitation waves as shown in Fig. 2A-Diii. For M island in WT condition (Fig. 2B), the re-entrant wave spontaneously terminated while sustained for M band distribution (Fig. 2A), which would be anticipated that the role of M island can terminate the re-entry, thus reduce the re-entrant lifespan (Fig. 3). However, for M island in SQT2 condition (Fig. 2D), the re-entrant wave sustained for longer time (Fig. 3), which would be anticipated that the role of M island can maintain the initiated re-entrant wave, thereby demonstrating an increased susceptibility to arrhythmia. The estimated minimal spatial length of S2 required for re-entry is shown in Fig. 4. Shortening of APD due to the KCNQ1 SQT2 mutation decreased the wavelength of the

ventricular excitation wave (WT-M band: 45 mm, WT-M island: 43 mm, HomKCNE1red-M band: 36 mm, HomKCNE1red-M island: 35 mm), thus reduced markedly the minimal length of S2. On the other hand, for M island, the minimal length was reduced both in WT and SQT2 conditions. This supports the notion that in M island tissue, re-entrant excitation waves can occur more easily than in M band tissue.

4. Discussion and conclusion

Increased spatial transmural heterogeneity of cardiac tissue in SQT2 condition causes to ventricular cells to repolarize at different rates, leading to function as a substrate for re-entry [4]. At present, there is no phenotypically accurate experimental model of SQT2. Moreover, the transmural wall is difficult to study the mechanisms of re-entrant excitation waves using only experimental methods. Consequently, this study was undertaken to investigate the functional effects of island-distribution of mid-cardiomyocytes on re-entrant

excitation waves in the short QT syndrome by using a computational model. This study showed how the island distribution of mid-cardiomyocytes provided a necessary substrate for the initiation, maintenance, and termination of transmural re-entry during the SQT2 syndrome condition. It was shown that in SQT2 re-entry was more easily initiated and sustained in the M island model than in the M band model. It illustrated the important role of spatial electrical heterogeneities of cardiac tissue in the increased incidence of ventricular fibrillation associated with short QT syndrome.

Acknowledgements

This study was supported in part by the National Natural Science Foundation of China (NSFC) under Grant No. 61572152 (to Henggui Zhang), No. 61571165 (Kuanquan Wang), and also supported by China Scholarship Council (CSC) (to Cunjin Luo).

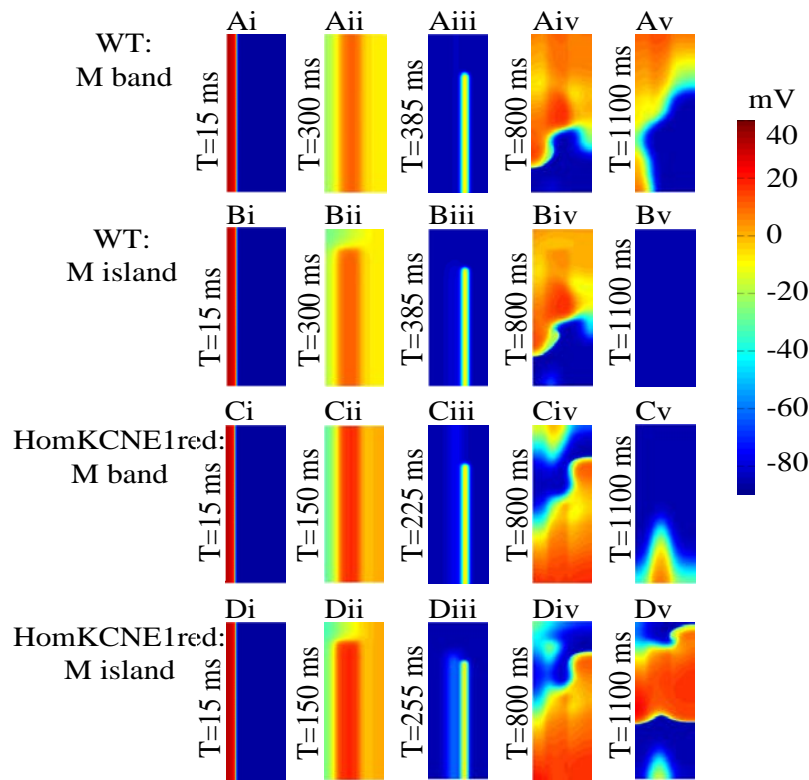


Fig. 2. Snapshots of initiation and conduction of re-entrant excitation waves in a 2D model of transmural ventricle tissue in WT (A, B) and SQT2 HomKCNE1red (C, D) conditions. M band distribution (A, C), M island distribution (B, D). Ai, Bi, Ci and Di: A planar conditioning wave generated by S1 at the base of ENDO part, which propagates towards EPI part. Snapshot taken at $t = 15$ ms from stimulation. Aii, Bii, Cii and Dii: Repolarization time of planar wave at $t = 300$ ms and $t = 150$ ms. Aiii, Biii, Ciii and Diii: S2 stimulus applied to the EPI part. Aiv, Biv, Civ and Div: Developed re-entrant excitation wave from the S2 stimulus at $t = 800$ ms. Av, Bv, Cv and Dv: Developed re-entrant excitation wave from the S2 stimulus at $t = 1000$ ms.

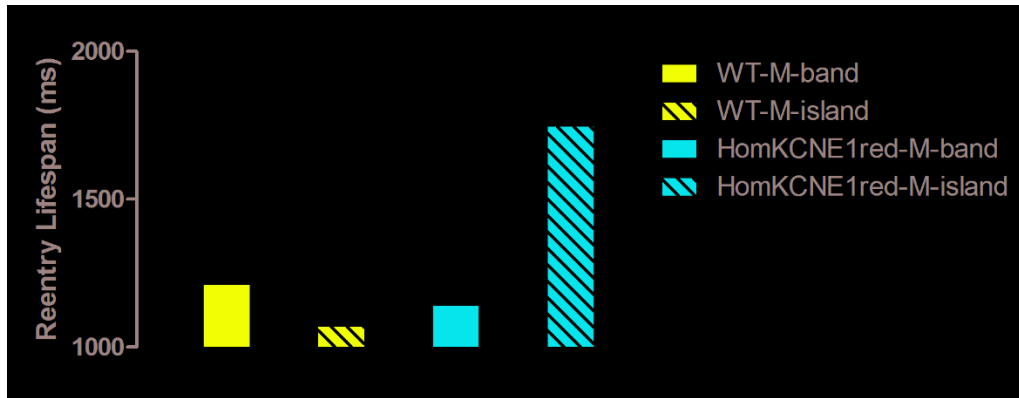


Fig. 3. Measured lifespan of re-entrant waves based on geometrical M band and M island distributions in WT and SQT2 HomKCNE1red conditions.

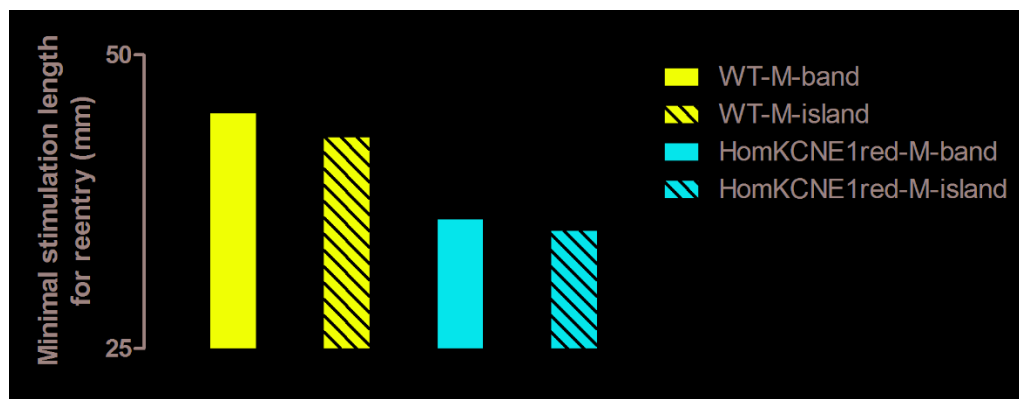


Fig. 4. The minimal spatial length of premature S2 stimulus that provides a large enough substrate for formulation of a re-entrant circuit based on geometrical M band and M island distributions for heterogeneous ventricular wall in WT and SQT2 HomKCNE1red conditions.

References

- [1] Henry H, Rappel WJ. The role of M cells and the long QT syndrome in cardiac arrhythmias: simulation studies of re-entrant excitations using a detailed electrophysiological model. *Chaos* 2004; 14(1): 172-82.
- [2] Bellocq C, van Ginneken AC, Bezzina CR, *et al.* Mutation in the KCNQ1 gene leading to the short QT-interval syndrome. *Circulation* 2004; 109(20), 2394-2397.
- [3] Hong K, Piper DR, Diaz-Valdecantos A, Brugada J, *et al.* KCNQ1 mutation responsible for atrial fibrillation and short QT syndrome in utero. *Cardiovasc. Res.* 2005; 68, 432-440.
- [4] Zhang H, Kharche S, Holden AV, Hancox JC. Repolarisation and vulnerability to re-entry in the human heart with short QT syndrome arising from KCNQ1 mutation— A simulation study. *Progress in Biophysics and Molecular Biology* 2008; 96, 112-131.
- [5] Ten Tusscher KH, Panfilov AV. Alternans and re-entrant breakup in a human ventricular tissue model. *Am J Physiol Heart Circ Physiol* 2006; 291:H1088-100.
- [6] Taggart P, Sutton PM, Opthof T, Coronel R, Trimlett R, Pugsley W, *et al.* Inhomogeneous transmural conduction during early ischemia in patients with coronary artery disease. *J Mol Cell Cardiol* 2000; 32:621-630.
- [7] Gima K, Rudy Y. Ionic current basis of electrocardiographic waveforms: a model study. *Circ Res* 2002; 90:889-896.
- [8] Henao OA, Ruiz CA, Ferrero JM. M-cell heterogeneity influence in arrhythmic pattern formation in sub-epicardial regional ischemia: a simulation study. *Computing in Cardiology* 2010; 37:189-192.
- [9] Akar FG, Yan GX, Antzelevitch C, Rosenbaum DS. Unique topographical distribution of M cells underlies reentrant mechanism of torsade de pointes in the long QT syndrome. *Circulation* 2002; 124:7-53.
- [10] Glukhov A, Fedorov V, Lou Q, Ravikumar V, *et al.* Transmural dispersion of repolarization in failing and nonfailing human ventricle. *Cir Res* 2010; 98:1-91.
- [11] Wang K, Luo C, Yuan Y, Lu W, Zhang H. Simulation of re-entrant wave dynamics in a 2D sheet of human ventricle with KCNJ2-linked variant 3 short QT syndrome. *Computing in Cardiology* 2014; 41: 61-64.
- [12] Wang K, Luo C, Wang W, Zhang H, Yuan Y. Simulation of KCNJ2-linked short QT syndrome in human ventricular tissue. *Computing in Cardiology* 2013; 40:349-352.

Address for correspondence.

Kuanquan Wang

wangkq@hit.edu.cn

Integrated laboratory building, Room 304,

School of Computer Science and Technology,

Harbin Institute of Technology, Harbin, 150001, China.